DOI: 10.1002/ejic.200900008

Structures and Physical Properties of Highly Conducting Single-Component Molecular Conductors Containing Se Atoms

Emiko Fujiwara,*[a] Biao Zhou,[b] Akiko Kobayashi,*[b] Hayao Kobayashi,[b] Yuichi Fujishiro,[c] Eiji Nishibori,[c] Makoto Sakata,[c] Shoji Ishibashi,[d] and Kiyoyuki Terakura[e]

Keywords: Selenium / Conducting materials / Nickel / Gold / Sulfur heterocycles

Single-component molecular conductors $[M(tmstfdt)_2]$ (M = Ni, Au; tmstfdt = trimethylenediselenadithiafulvalenedithiolate) substituted with Se atoms are prepared and found to be isostructural with $[M(tmdt)_2]$ (M = Ni, Au; tmdt = trimethylenetetrathiafulvalenedithiolate). Measurements of the electrical conductivity and magnetic susceptibility of $[Ni(tmstfdt)_2]$ show that it has essentially metallic properties down to low temperatures. The resistivity measurements of $[Au(tmstfdt)_2]$ suggest it undergoes a metal-insulator phase transition at around 100 K. Magnetic susceptibility and ESR measurements of $[Au(tmstfdt)_2]$ indicate that it undergoes a magnetic transition at around 5 K, which is much lower than the antiferromagnetic (AF) phase-transition temperature of $[Au(tmdt)_2]$ (110 K).

Introduction

Novel molecular conducting systems have attracted considerable attention recently, and the number of interesting reports on such molecular systems is rapidly increasing.[1] Among these systems, molecular crystals consisting of single-component molecules have opened up a new route to molecule-based electronic conductors. The single-component molecular crystal consisting of the neutral metal complex $[Ni(tmdt)_2]$ (tmdt = trimethylenetetrathiafulvalenedithiolate) with extended-TTF (TTF = tetrathiafulvalenedithiolate) ligands is the first single-component molecular metal in which metal electrons are automatically generated by the self-assembly of neutral molecules. This molecular crystal exhibits stable metallic behaviour down to 0.6 K.[2,3] Furthermore, the existence of 3D electron and hole Fermi surfaces (FS) was confirmed by the de Haas–van Alphen (dHvA) effect, which provided the first concrete evidence for the existence of FS in crystals consisting of single-component molecules.[4] Recent, detailed measurements of the resistivity and magnetoresistance of $[Ni(tmdt)_2]$ have shown that the resistivity has a T^2 dependence below 30 K,[5] which cannot be explained by a simple Fermi-liquid picture. The highly isotropic positive magnetoresistance below 4.2 K indicates the possibility of a contribution from a spin-orbit interaction. In contrast to the dHvA effect, no oscillatory magnetoresistance was observed up to magnetic field strengths of 33 T and down to 0.7 K, probably because of the very low resistivity of $[Ni(tmdt)_2]$ and the effective mass of the complex being similar to that of a free electron.[5]

Since the discovery of $[Ni(tmdt)_2]$, various other metal complexes with extended-TTF-type ligands have been synthesised,[6–10] with the gold complex being particularly interesting. In contrast to neutral bis(dithiolato)nickel complexes, neutral bis(dithiolato)gold complexes have one unpaired electron per complex, which means they may exhibit attractive electromagnetic properties.[2,8–10] ESR spectra and magnetic susceptibility measurements, for instance, have revealed that $[Au(tmdt)_2]$ undergoes an antiferromagnetic (AF) phase transition at around 110 K,[11,12] and a ^1H NMR study has shown a steep increase in the NMR linewidth and a peak due to $1/T_1$ at around 110 K.[13] These observations provide microscopic evidence for a magnetic phase transition. The observed variation of $1/T_1$ indicates a highly correlated nature of the metallic phase.[13] The resistivity of $[Au(tmdt)_2]$ in the compact polycrystalline state has a non-metallic temperature dependence ($\sigma_{RT} \approx 50\ S\,cm^{-1}$).[12] On the other hand, the resistivity of $[Au(tmdt)_2]$ crystals grown on finely patterned interdigi-

[a] Research Centre for Spectrochemistry, Graduate School of Science, The University of Tokyo,
Hongo, Bunkyo-ku, Tokyo 113-0033, Japan
[b] Department of Chemistry, College of Humanities and Sciences, Nihon University,
Sakurajosui, Setagaya-ku, Tokyo 156-8550, Japan
Fax: +81-3-5317-9433
E-mail: akoba@chs.nihon-u.ac.jp
[c] Department of Applied Physics, Nagoya University,
Nagoya 464-8603, Japan
[d] Research Institute for Computational Sciences (RICS), National Institute of Advanced Industrial Science and Technology (AIST),
1-1-1 Umezono, Tsukuba, Ibaraki 305-8568, Japan
[e] Research Centre for Integrated Science (RCIS), Japan Advanced Institute of Science and Technology (JAIST),
1-1 Asahidai, Nomi, Ishikawa 923-1292, Japan

tated electrodes separated by 5–10 μm has shown that $[Au(tmdt)_2]$ is metallic down to 4 K.[14] The conductivity of extremely small (ca. 30 μm) $[Au(tmdt)_2]$ crystals also reveals that the system is metallic down to 4.2 K.[15] In this experiment, the slope of the temperature-dependence curves of resistivities was found to change at around 110 K. This change was not observed in previous measurements in which compressed pellet samples[12] and microcrystals were used.[14] In addition, the results of ab initio plane-wave pseudopotential calculations of $[Au(tmdt)_2]$ have indicated that the nesting of the FS is not perfect and that FS pockets exist at temperatures below the AF phase-transition temperature.[16] From the above mentioned data, $[Au(tmdt)_2]$ was concluded to be the first AF molecular metal with T_N above 100 K, and it was found to be a novel metal in which π electrons and magnetic order coexist down to low temperatures.

The introduction of heavier chalcogen atoms into molecular conducting systems is usually expected to increase intermolecular interactions in the solid state and result in the widening of conduction bands. For example, the room-temperature conductivity of a compressed pellet sample of the single-component nickel complex substituted with two TTF diselenolate ligands and four ethylthio groups is around 60 times higher than that of its sulfur analogue.[17] On the other hand, substitution of Se atoms for S atoms produces larger lattice constants, which tends to make the system poorly conducting. From this perspective, single-component molecular conductors substituted with Se atoms may be of special interest, therefore we have focused on the introduction of STF (diselenadithiafulvalene) frameworks into $[M(tmdt)_2]$ (M = Ni, Au) in order to obtain strong intermolecular networks via S(Se)···S(Se) contacts. Herein we report the preparation, crystal-structure determination, physical properties, and band-structure calculations of nickel and gold complexes with two trimethylenediselenadithiafulvalenedithiolate (tmstfdt) ligands {$[M(tmstfdt)_2]$; M = Ni **1**, Au **2**}; these complexes have four Se atoms on the outer sides of the ligands.

Results and Discussion

Syntheses

Complexes **1** and **2** were synthesised as shown in Scheme 1. The precursor of the ligand moiety [4,5-bis(2′-cyanoethylthio)-4′,5′-trimethylene-STF (**5**)] was synthesised by a cross-coupling reaction between 4,5-trimethylene-1,3-diselenol-2-one (**3**)[18] and 4,5-bis(2′-cyanoethylthio)-1,3-dithiol-2-one (**4**)[19] in dry trimethylphosphite at 110 °C. The reaction mixture was evaporated to dryness in vacuo, and the resultant red oil was purified by column chromatography (silica gel, dichloromethane). The product was obtained as air-stable orange crystals in 12% yield after recrystallisation from dichloromethane/*n*-hexane. The tetramethylammonium salts $(Me_4N)_2[Ni(tmstfdt)_2]$ (**6**) and $(Me_4N)[Au(tmstfdt)_2]$ (**7**) were synthesised in an inert atmosphere following a procedure reported in the literature.[2,3] Deprotection of **5** with a 25 wt.-% methanol solution of tetramethylammonium hydroxide in dry THF at room temperature yielded the bis(tetramethylammonium)dithiolate ligand $(Me_4N)_2$tmstfdt as a reddish air-unstable precipitate. Subsequently, successive treatment with a MeOH solution of $NiCl_2·6H_2O$ or $HAuCl_4·4H_2O$ between –78 °C and room temperature afforded complexes **6** and **7**, respectively. Microcrystals of **1** were grown on anode electrodes by the electrochemical oxidation of **6** in the presence of $nBu_4N·ClO_4$ in THF, while those of **2** were grown by the electrochemical oxidation of **7** in the presence of $nBu_4N·PF_6$ in acetonitrile (MeCN); this growth process was completed within approximately 3–4 weeks.

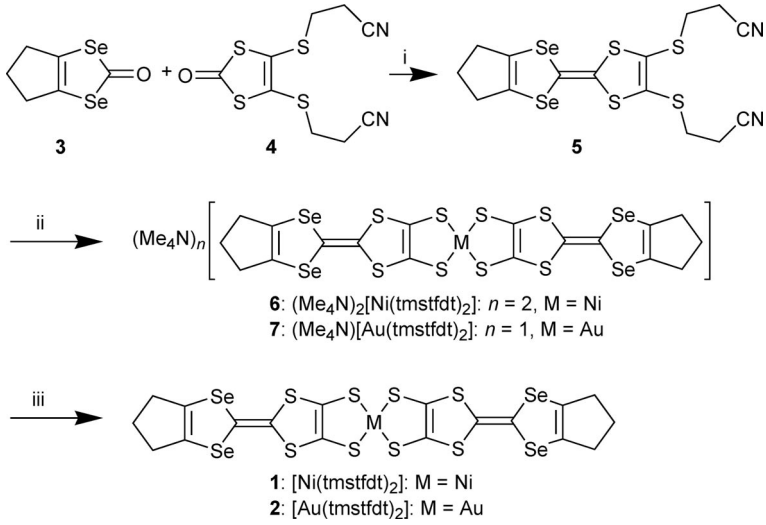

Scheme 1. Reagents and conditions: (i) $P(OMe)_3$, 110 °C, 1.5 h; (ii) 25 wt.-% tetramethylammonium hydroxide in MeOH (4 equiv.), dry THF, room temperature, 30 min, then $NiCl_2·6H_2O$ (0.5 equiv.) or $HAuCl_4·4H_2O$ (0.5 equiv.), –78 °C to room temperature, overnight; (iii) electrochemical oxidation in THF or MeCN containing $nBu_4N·ClO_4$ or $nBu_4N·PF_6$ as supporting electrolytes, respectively, at room temperature; 0.3 or 0.5 μA.

Crystal Structure Analyses

X-ray structure analyses of single crystals of **1** and **2** were unsuccessful owing to the extremely small sizes of the obtained crystals. Therefore, in order to determine their crystal structures, synchrotron radiation X-ray powder diffraction experiments were performed using an imaging plate detector and a large Debye–Scherrer camera at the BL02B2 beamline at SPring-8. The ideal X-ray powder patterns of microcrystals of **1** and **2** showed that they are isostructural with $[M(tmdt)_2]$ (M = Ni, Au).[2,3,11] Thus, the structures of **1** and **2** were analysed by using the MEM/Rietveld method, which can be used to carry out self-consistent iterative analysis; this method is a combination of the maximum entropy method (MEM) and Rietveld analysis.[20] As shown in Figure 1 (a and b), each crystal of **1** and **2** has a very simple structure with only one $[M(tmstfdt)_2]$ (M = Ni, Au) molecule in the unit cell and all the central metal atoms located at the inversion centre of the lattice points. The interplanar distances between the molecules are short, at 3.55 (M = Ni) and 3.49 Å (M = Au) in the [111] direction and 3.66 (M = Ni) and 3.77 Å (M = Au) in the [101] direction. The intermolecular S(Se)···S(Se) contacts were observed to be shorter than the sum of the van der Waals radii for both **1** and **2**. The shortest intermolecular S···S distance in both salts was 3.49 Å in the [100] direction. The existence of numerous three-dimensional short intermolecular S(Se)···S(Se) contacts suggests that the $[M(tmstfdt)_2]$ (M = Ni, Au) molecules are assembled to form simple and dense 3D structures since S(Se)···S(Se) interactions are stronger than van der Waals interactions in the crystal.

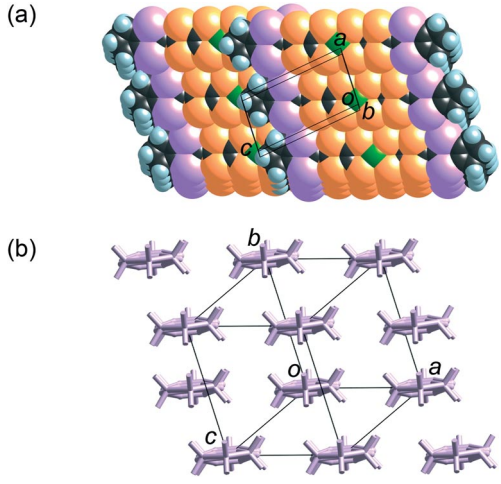

Figure 1. (a) Crystal structure and molecular packing of **1**. (b) Packing mode of **1** viewed along the molecular long axis. Complexes **1** and **2** are isostructural.

Electrical Properties

Resistivity measurements were carried out by the conventional four-probe method from room temperature to 4.2 K and from room temperature to 10 K on compressed pellet samples of **1** and **2**, respectively. The room-temperature conductivities of **1** and **2** were fairly high (σ_{RT} = 100 S cm^{-1} for M = Ni and 11 S cm^{-1} for M = Au), even for measurements carried out on compacted powder samples. On the basis of these observations, single crystals of **1** and **2** were expected to be fairly good conductors. Parts (a) and (b) of Figure 2 show the temperature-dependence of the resistivities of compressed pellet samples of **1** and **2**. The resistivity of **1** decreases with a decrease in temperature down to around 50 K and then increases very slowly with a further decrease in temperature. Complex **1** continues to show fairly high conductivity even at 4.2 K ($\sigma_{4.2K} \approx \sigma_{RT}$), thus suggesting that it is essentially a metallic complex down to

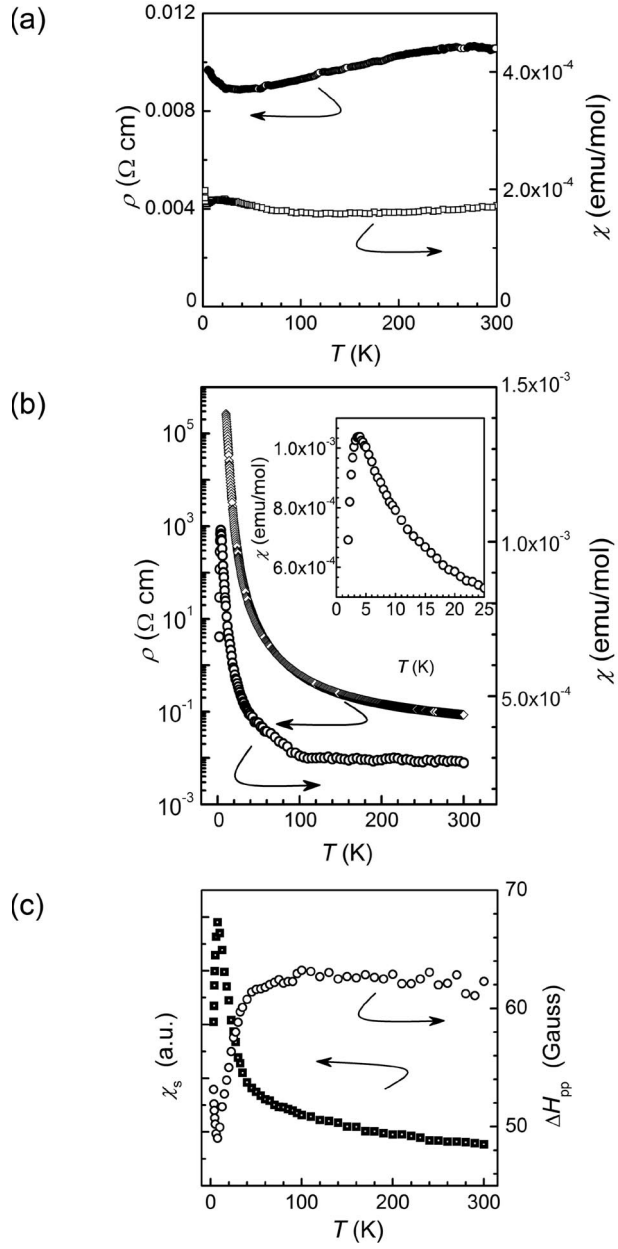

Figure 2. (a) Temperature-dependence of the resistivities (ρ) and magnetic susceptibilities (χ) for **1**. (b) Temperature-dependence of ρ and χ for **2**. The resistivities of **1** and **2** were measured using compressed pellet samples. (c) Temperature-dependence of χ_s and ΔH_{pp} estimated from the ESR measurements with **2**.

the lowest temperature region. On the other hand, the resistivity of **2** increases gradually with a decrease in temperature, but the activation energy of its semiconducting behaviour is very low (0.028 eV, 200–300 K; 0.015 eV, 20–50 K).

Magnetic Properties

Figure 2 [parts (a) and (b)] show the temperature-dependence of the magnetic susceptibilities of **1** and **2**. The magnetic susceptibilities were measured using a SQUID magnetometer at 10 kOe in the temperature range 2.0–300 K. The data obtained after correction by subtracting the diamagnetic contribution ($^{dia}\chi = -3.35 \times 10^{-4}$ emu mol^{-1}) and the small low-temperature Curie term revealed that the magnetic susceptibility of **1** is almost constant in the above-mentioned temperature range. These corrections had to be made due to the presence of paramagnetic impurities and/or lattice defects. The results of the measurements indicate the Pauli-paramagnetism of the metal electrons. This is consistent with the stable metallic conduction behaviour of **1**. The magnetic susceptibility of **2** also shows Pauli-like paramagnetism down to around 100 K after subtraction of the diamagnetic contribution ($^{dia}\chi = -3.56 \times 10^{-4}$ emu mol^{-1}) and Curie impurities of about 1% from the measured data. Despite the weak semiconducting behaviour observed for the compressed pellet samples of **2**, the constant susceptibilities above 100 K and fairly high conductivity ($\sigma_{RT} \approx 10$ S cm^{-1}) indicate that **2** is essentially metallic at least above about 100 K. On the other hand, the paramagnetic susceptibilities of **1** and **2** at around room temperature ($\chi_{300K} = 1.8 \times 10^{-4}$ emu mol^{-1} for **1** and 3.0×10^{-4} emu mol^{-1} for **2**) are slightly smaller than those of their sulfur analogues [M(tmdt)$_2$] (3.1×10^{-4} emu mol^{-1} for M = Ni and 3.8×10^{-4} emu mol^{-1} for M = Au).[2,3,11]

The ESR spectra of a polycrystalline sample of **2** were recorded with a Bruker ESP300E ESR spectrometer. As shown in Figure 2c, the peak-to-peak linewidths (ΔH_{pp}) for **2** are almost constant, with a value of around 62 G above about 100 K. The ΔH_{pp} values of this system, however, show a slight decrease with a decrease in temperature below this temperature and increase with a decrease in temperature below about 5 K. In contrast, the spin susceptibility (χ_s) of **2** increases as the temperature decreases from 300 K to the low temperature region, especially below 35 K. A sudden decrease in χ_s was observed below about 5 K. This anomaly was also confirmed by the SQUID magnetic susceptibility measurements, as shown in the inset of Figure 2b. This magnetic behaviour suggests a magnetic transition in **2** at around 5 K. [Au(tmdt)$_2$] undergoes an AF transition at 110 K, which has been confirmed by several experiments.[2,11–13] In contrast to [Au(tmdt)$_2$], which exhibits a transition from a high temperature metallic state with constant susceptibility to an antiferromagnetic metal state at 110 K, **2** shows a susceptibility peak at around the magnetic transition temperature. This indicates that the nature of the magnetic transition in **2** is different from that in [Au(tmdt)$_2$].

Band-Structure Calculations

Ab initio band-structure calculations for **1** and **2** were carried out on the basis of the density-functional theory using our in-house computational code QMAS (Quantum MAterials Simulator).[21] The projector augmented-wave (PAW) method was used.[22–24] The exchange and correlation energies for the electrons were calculated by using the generalized gradient approximation (GGA)[25] in combination with partial-core correction.[26] The plane-wave cut-off energy was set to 20 hartree. For non-magnetic self-consistent calculations of the solid states of **1** and **2**, 128 k points were used in one-half of the Brillouin zone for **1** and **2**. Figure 3a shows the band dispersion of **1**. The energy zero corresponds to the Fermi level. The electronic structure of **1** is very similar to that of [Ni(tmdt)$_2$],[16,27] and some band widths of **1** are wider than those of [Ni(tmdt)$_2$]. This is consistent with our original expectation that substitution of Se for S leads to an increase in band width. However, the present situation seems not simple. For example, the width of the highest band shown in Figure 3a is slightly narrower than the corresponding one for [Ni(tmdt)$_2$]. As shown in the Experimental Section, the tmstfdt salt has larger lattice parameters than those of the tmdt salt. Generally, the larger the lattice parameter, the narrower the band width along its direction. On the other hand, the large Se orbital is expected to broaden the widths of bands where the Se contribution is significant. If all the S atoms are substituted with Se atoms, the latter effect will be predominant. For the tmstfdt case, only the outermost S atoms are substituted. Since the molecular orbital contributing to the highest band in Figure 3a has no significant contribution from Se atoms, the lattice expansion plays a predominant role and the band width became narrower for the tmstfdt case, which is consistent with the poorer conducting properties of **2**. Figure 3 (b and c) shows the electron density of states (DOS) in the vicinity of the Fermi level for **1** and the FS of **1**, respectively. Two bands in **1** are clearly observed to cross the Fermi level, as previously reported for [Ni(tmdt)$_2$].[16,28] The HOMO and LUMO states of neighbouring molecules hybridize strongly with each other to yield two HOMO–LUMO composite bands.[28,29] This serves as conclusive evidence to confirm the metallic nature of [Ni(tmdt)$_2$] and **1**. The FS of **1** is very similar to that of [Ni(tmdt)$_2$].

In the case of [Au(tmdt)$_2$], one additional electron shifts the Fermi level upward and only one band crosses it. The energy level of the SOMO+1 (i.e., LUMO) decreases close to that of the SOMO.[28] Note that the SOMO+1 in the Au salt corresponds to the LUMO+1 in the Ni salt from which the narrow one-dimensional isolated band centred around 0.8 eV in Figure 3b is formed. Because of the smaller energy separation between the SOMO and SOMO+1 in [Au(tmdt)$_2$], the corresponding band coming from SOMO+1 is no longer isolated and hybridized with the lower band. The degree of this hybridisation seems to be slightly weaker in **2** than in [Au(tmdt)$_2$], although the DOSs for the two materials are quite similar. [Au(tmdt)$_2$] un-

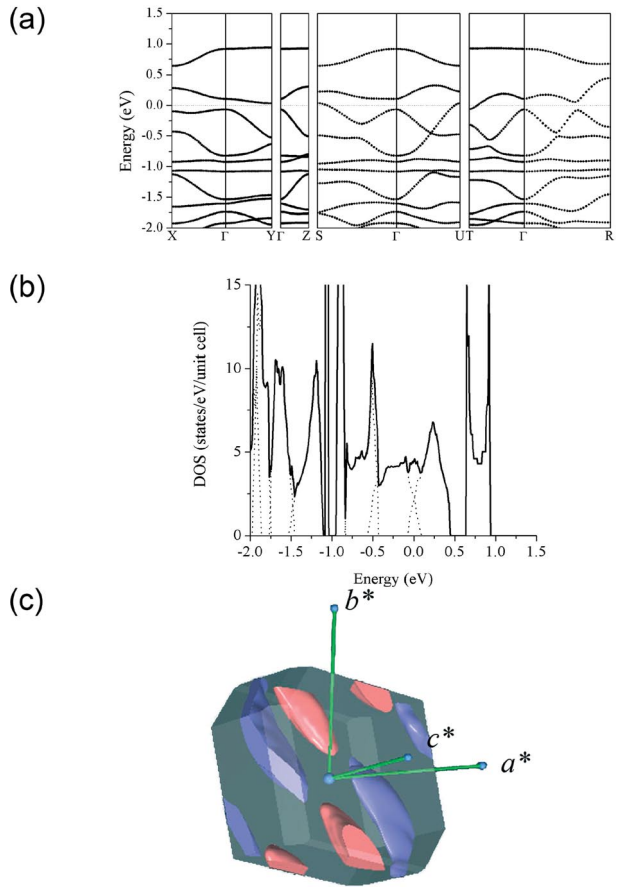

Figure 3. (a) Band dispersion of **1**. (b) Electron DOS of **1**. (c) Calculated 3D electron (red) and hole (blue) FS of **1**.

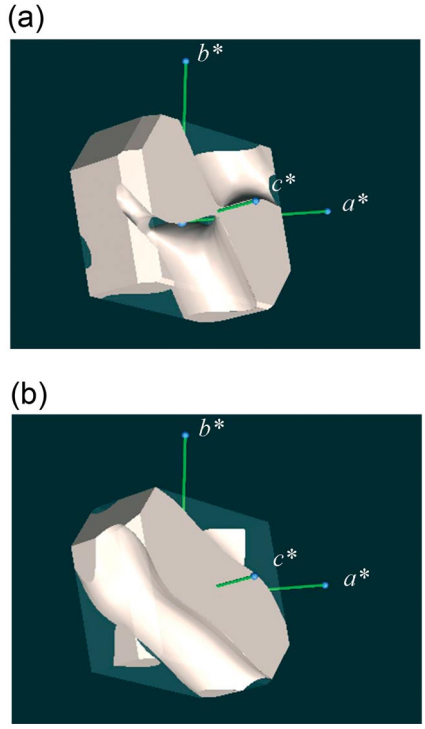

Figure 4. FS of $[Au(tmdt)_2]$ (a) and $[Au(tmsftdt)_2]$ (b), which are plotted as hole surfaces.

dergoes a magnetic phase transition at around 110 K, and antiferromagnetic ordering has been observed in several experiments.[11–13] In the case of **2**, Figure 2 (b and c) shows the occurrence of a magnetic transition at around 5 K. As described earlier, the geometrical factor in the generalized susceptibility χ_o calculated for $[Au(tmdt)_2]$ has a distinct peak at $q = a^*/2$, where a^* is one of the reciprocal lattice vectors. No such peak is observed in the case of **2**.[28] This observation is consistent with the experimental results, which show that unlike $[Au(tmdt)_2]$, **2** does not undergo an AF phase transition at high temperatures. Figure 4 shows the FS of $[Au(tmdt)_2]$ and **2**. The calculated FS is consistent with Pauli-like constant susceptibility of **2** at room temperature.

Conclusions

The complexes $[M(tmstfdt)_2]$ (M = Ni **1** and Au **2**) have been confirmed to be isostructural with $[M(tmdt)_2]$ (M = Ni, Au) on the basis of synchrotron-radiation powder X-ray diffraction data. Complexes **1** and **2** show fairly large room-temperature conductivities, even in measurements carried out using compressed pellet samples. In particular, **1** exhibits metallic conduction behaviour down to around 50 K and retains its high conductivity even at 4.2 K [$\sigma_{4.2K} \approx \sigma_{RT}$]. Complex **1** essentially remains metallic down to very low temperatures, in agreement with the Pauli-paramagnetic behaviour of its magnetic susceptibilities. Complex **1** was confirmed to be metallic (similar to $[Ni(tmdt)_2]$) by the existence of its 3D electron and hole FS, as determined by band-structure calculations. Substitution with heavier Se atoms leads to an increase in the intermolecular interactions in crystals of **1** because of the increased orbital size of the Se atom. Although all the data were obtained using powder samples, we firmly believe that the newly synthesised complex **1** is a unique 3D single-component molecular metal incorporating Se-containing STF ligands. $[Au(tmsfdt)_2]$ (**2**) also shows essentially metallic behaviour down to 100 K, below which the magnetic susceptibility increases rapidly down to about 5 K. This complex then undergoes a magnetic transition. These features of **1** and **2** show that the Se substitution effect is not simple. The results of ab initio band structure calculations are consistent with the stable metallic state of **1** and also suggest a narrow metal band for **2**.

Experimental Section

General Procedures: 4,5-Trimethylene-1,3-diselenol-2-one (**3**)[18] and 4,5-bis(2′-cyanoethylthio)-1,3-dithiol-2-one (**4**)[19] were synthesised using the methods described in the literature. Trimethylphosphite was vacuum distilled from sodium and stored under argon. THF was freshly distilled from sodium and benzophenone under argon prior to use. MeOH was distilled from magnesium ethoxide under argon. MeCN was distilled in the presence of calcium hydride under argon. The supporting electrolytes were recrystallised several times with ethanol and dried in vacuo. All other reagents were used without purification. Melting points were determined

using a Yanako MP-J3 micro melting-point apparatus and were not corrected. Microanalyses were performed by the Organic Elemental Analysis Centre, Department of Chemistry, School of Science, The University of Tokyo. ^{1}H NMR spectra were recorded with a JEOL JNM-LA300SXA FT-NMR system; chemical shift values are expressed in parts per million (ppm) relative to the internal standard tetramethylsilane (TMS). Mass spectra were obtained using a TOF mass spectrometer, Shimadzu/Kratos AXIMA-CFR Plus, and IR spectra were obtained using a Shimadzu FTIR-8400S spectrometer.

Synthesis of 4,5-Bis(2′-cyanoethylthio)-4′,5′-trimethylene-STF (5): Compounds **3** (12.0 mmol) and **4** (18.0 mmol) were dissolved in dry trimethylphosphite (190 mL) under argon and the resulting pale-yellow solution slowly heated to 110 °C for 1.5 h. It was then cooled to room temperature and the solvent evaporated under reduced pressure. The resulting red oil was purified by column chromatography (silica gel, dichloromethane). The product obtained by chromatography was recrystallised from dichloromethane/*n*-hexane to afford air-stable, orange crystals of **5** in 12% yield. M.p. 150.5–152.6 °C (dec.). IR (KBr): $\tilde{\nu}$ = 2957, 2928, 2841, 2827, 2255, 1435, 1425, 1323, 1229, 1117, 989, 885, 758, 717 cm^{-1}. ^{1}H NMR ($CDCl_3$, 300 MHz): δ = 2.325–2.425 (m, J = 7.5 Hz, 2 H, CH_2), 2.597 (t, J = 6.9 Hz, 4 H, $H_2CC{=}CCH_2$), 2.736 (t, J = 7.2 Hz, 4 H, $2CH_2CN$), 3.083 (t, J = 6.9 Hz, 4 H, $2SCH_2$) ppm. MS: m/z 510 [M$^+$]. $C_{15}H_{14}N_2S_4Se_2$ (508.45): calcd. C 35.43, H 2.78, N 5.51.; found C 35.21, H 2.50, N 5.69.

Synthesis of Nickel Complexes 6 and 1: Compound **5** (0.125 mmol) was dissolved in dry THF (10 mL) and a 25 wt.-% MeOH solution of $Me_4N{\cdot}OH$ (0.510 mmol) was added to this solution at room temperature. $(Me_4N)_2$tmstfdt was obtained as an air-unstable reddish precipitate. A solution of $NiCl_2{\cdot}6H_2O$ (0.065 mmol) in MeOH (2.5 mL) was added to the system at –78 °C and the reaction mixture warmed to room temperature to give reddish brown $(Me_4N)_2$-[Ni(tmstfdt)$_2$] (**6**). Electrocrystallisation was carried out under argon in a standard H-type cell without a glass frit using two platinum electrodes of 1 mm diameter. Complex **6** (ca. 0.01 mmol) was subjected to electrochemical oxidation in nBu$_4$N·ClO$_4$ (0.2 mmol) and THF (20 mL). After passing a current of 0.3 μA through the circuit for 3–4 weeks, black microcrystals of **1** were obtained on the platinum electrode; these microcrystals were stable in air and insoluble in conventional organic solvents. Elemental analysis of **1**. $C_{18}H_{12}NiS_8Se_4$ (859.32): calcd. C 25.16, H 1.41, N 0.00; found C 24.86, H 1.71, N 0.00.

Synthesis of Gold Complexes 7 and 2: (Me_4N)[Au(tmstfdt)$_2$] (**7**) was synthesised via the intermediate compound $(Me_4N)_2$tmstfdt following a method almost identical to that used for the synthesis of **6**. A 25 wt.-% MeOH solution of tetramethylammonium hydroxide (0.512 mmol) in dry THF (10.0 mL) and a solution of $HAuCl_4{\cdot}4H_2O$ (0.064 mmol) in dry MeOH (2.5 mL) were used as the starting materials to afford **7** in the form of air-unstable brown microcrystals. Microanalysis and estimation of the yield could not be performed because of this instability. Complex **7** (ca. 0.01 mmol) was subjected to electrochemical oxidation in nBu$_4$N·PF$_6$ (0.2 mmol) and MeCN (20 mL). After applying a current of 0.5 μA in the circuit for 3–4 weeks, black microcrystals of **2** were obtained on the platinum electrode; these microcrystals were stable in air and insoluble in conventional organic solvents. Elemental analysis of **2**. $C_{18}H_{12}AuS_8Se_4$ (997.58): calcd. C 21.67, H 1.21, N 0.00; found C 21.35, H 1.48, N 0.00.

X-ray Powder Diffraction for Neutral Complexes 1 and 2: Synchrotron radiation X-ray powder diffraction experiments were performed on **1** and **2** to obtain information on their crystal structures.

Crystallographic Data for [Ni(tmstfdt)$_2$] 1: $C_{18}H_{12}NiS_8Se_4$, triclinic, space group $P\bar{1}$, a = 6.5287(1), b = 7.5221(2), c = 12.1628(2) Å, α = 90.794(2)°, β = 96.848(2)°, γ = 103.799(3)°, V = 575.38(4) Å^3, Z = 1, R_{wp} = 0.079, R_I = 0.130.

Crystallographic Data for [Au(tmstfdt)$_2$] 2: $C_{18}H_{12}AuS_8Se_4$, triclinic, space group $P\bar{1}$, a = 6.5220(7), b = 7.5032(3), c = 12.303(2) Å, α = 90.26(1)°, β = 96.85(2)°, γ = 103.43(2)°, V = 581.1(2) Å^3, Z = 1, R_{wp} = 0.016, R_I = 0.067.

The experiments were carried out using imaging plate detectors and a large Debye–Scherrer camera at the BL02B2 beamline at SPring-8. The wavelength of the incident X-rays used for **1** and **2** was 1.0007 Å. The exposure times were 150 and 30 min for **1** and **2**, respectively. The ideal X-ray powder pattern for **1** was obtained in steps of 0.01° for 2θ values ranging from 2.5° to 45.05°. The ideal X-ray powder pattern for **2** was obtained in steps of 0.01° for 2θ values ranging from 3.5° to 40.0°. The structures of **1** and **2** were solved by the MEM/Rietveld method, which can be used to carry out self-consistent iterative analysis; this method is a combination of the maximum entropy method (MEM) and Rietveld analysis.[20]

CCDC-706678 (for **1**) and -706677 (for **2**) contain the supplementary crystallographic data for this paper. These data can be obtained free of charge from the Cambridge Crystallographic Data Centre at www.ccdc.cam.ac.uk/data_request/cif.

Electrical Resistivity Measurements: The electrical resistivities of **1** and **2** were measured by the four-probe technique using compressed pellet samples. Measurements were performed using a Huso Electro Chemical System HECS 994C-1 multichannel four-terminal conductometer. Resistivities were measured down to 4.2 and 10 K for **1** and **2**, respectively. Electrical contacts were achieved using gold paste and gold wires (diameter: 15 μm).

Static Magnetic Susceptibility Measurements: Static magnetic susceptibility (χ) measurements for complexes **1** (2.45×10^{-2} mmol) and **2** (4.83×10^{-3} mmol) were performed in the temperature range 2.0–300 K using a Quantum Design MPMS-7XL SQUID magnetometer. The applied magnetic field was 10 kOe. The samples were wrapped in a clean aluminium foil. The magnetic susceptibility of the foil was measured separately and subtracted from the total values. The diamagnetic contribution was calculated using Pascal's constants ($^{dia}\chi = -3.35 \times 10^{-4}$ and -3.56×10^{-4} emu mol^{-1} for **1** and **2**, respectively).

ESR Spectrum Measurements: ESR spectra of the polycrystalline samples of **2** in an evacuated quartz tube were measured using a Bruker ESP300E ESR spectrometer in the temperature range 3.3–300 K. The applied microwave power and modulation field were 1.0 mW and 9.5 G, respectively.

MO and Band-Structure Calculations: The calculations were carried out using the in-house computational code QMAS (Quantum MAterials Simulator).[21] The projector augmented-wave (PAW) method was adopted.[22–24] The exchange and correlation energies for the electrons were calculated by using the generalized gradient approximation (GGA)[25] along with partial-core correction.[26]

Acknowledgments

The authors are grateful to Mr. Y. Okano of IMS for valuable discussions. Financial support for this study was provided by a Grant-in-Aid for Scientific Research (B) from the Ministry of Education, Culture, Sports, Science and Technology, Japan (grant no. 20350069). Synchrotron-radiation experiments were performed at

the BL02B2 beamline at SPring-8 with the approval of the Japan Synchrotron Radiation Research Institute (JASRI).

[1] Recent physical and chemical studies on molecular conductors have been reviewed in a *thematic issue* of *Chem. Rev.* (**2004**, *104*; Molecular Conductors, edited by P. Batail), and *J. Phys. Soc. Jpn.* **2006**, 75 (Organic Conductors, edited by S. Kagoshima, K. Kanoda, T. Mori).

[2] A. Kobayashi, E. Fujiwara, H. Kobayashi, *Chem. Rev.* **2004**, *104*, 5243–5264.

[3] a) H. Tanaka, Y. Okano, H. Kobayashi, W. Suzuki, A. Kobayashi, *Science* **2001**, *291*, 285–287; b) A. Kobayashi, H. Tanaka, H. Kobayashi, *J. Mater. Chem.* **2001**, *11*, 2078–2088; c) I. Malfant, K. Rivasseau, J. Fraxedas, C. Faulmann, D. de Caro, L. Valade, L. Kaboub, J. M. Fabre, F. Senocq, *J. Am. Chem. Soc.* **2006**, *128*, 5612–5613.

[4] H. Tanaka, M. Tokumoto, S. Ishibashi, D. Graf, E. S. Choi, J. S. Brooks, S. Yasuzuka, Y. Okano, H. Kobayashi, A. Kobayashi, *J. Am. Chem. Soc.* **2004**, *126*, 10518–10519.

[5] S. Yasuzuka, H. Tanaka, M. Tokumoto, D. Graf, E. S. Choi, J. S. Brooks, H. Kobayashi, A. Kobayashi, *J. Phys. Soc. Jpn.* **2008**, *77*, 034709/5.

[6] J. P. M. Nunes, M. J. Figueira, D. Belo, I. C. Santos, B. Ribeiro, E. B. Lopes, R. T. Henriques, J. V. Gancedo, J. Veciana, C. Rovira, M. Almeida, *Chem. Eur. J.* **2007**, *13*, 9841–9849.

[7] H.-R. Wen, C.-H. Li, Y. Song, J.-L. Zuo, B. Zhang, X.-Z. You, *Inorg. Chem.* **2007**, *46*, 6837–6839.

[8] A. J. Schultz, H. H. Wang, L. C. Soderholm, T. L. Sifter, J. M. Williams, K. Bechgaard, M.-H. Whangbo, *Inorg. Chem.* **1987**, *26*, 3757–3761.

[9] N. C. Schiødt, T. Bjørnholm, K. Bechgaard, J. J. Neumeier, C. Allgeier, C. S. Jacobsen, N. Thorup, *Phys. Rev. B* **1996**, *53*, 1773–1778.

[10] D. Belo, H. Alves, E. B. Lopes, M. T. Duarte, V. Gama, R. T. Henriques, M. Almeida, A. Pérez-Benítez, C. Rovira, J. Veciana, *Chem. Eur. J.* **2001**, *7*, 511–519.

[11] W. Suzuki, E. Fujiwara, A. Kobayashi, Y. Fujishiro, E. Nishibori, M. Takata, M. Sakata, H. Fujiwara, H. Kobayashi, *J. Am. Chem. Soc.* **2003**, *125*, 1486–1487.

[12] B. Zhou, M. Shimamura, E. Fujiwara, A. Kobayashi, T. Higashi, E. Nishibori, M. Sakata, H.-B. Cui, K. Takahashi, H. Kobayashi, *J. Am. Chem. Soc.* **2006**, *128*, 3872–3873.

[13] Y. Hara, K. Miyagawa, K. Kanoda, M. Shimamura, B. Zhou, A. Kobayashi, H. Kobayashi, *J. Phys. Soc. Jpn.* **2008**, *77*, 053706/4.

[14] H. Tanaka, S. Hara, M. Tokumoto, A. Kobayashi, H. Kobayashi, *Chem. Lett.* **2007**, *36*, 1006–1007.

[15] H.-B. Cui, J. S. Brooks, private communication.

[16] S. Ishibashi, H. Tanaka, M. Kohyama, M. Tokumoto, A. Kobayashi, H. Kobayashi, K. Terakura, *J. Phys. Soc. Jpn.* **2005**, *74*, 843–846.

[17] K. Ueda, Y. Kamata, M. Iwamatsu, T. Sugimoto, H. Fujita, *J. Mater. Chem.* **1999**, *9*, 2979–2983.

[18] a) Y. Okano, H. Sawa, S. Aonuma, R. Kato, *Chem. Lett.* **1993**, 1851–1853; b) Y. Okano, H. Sawa, S. Aonuma, R. Kato, *Synth. Met.* **1995**, *70*, 1161–1162.

[19] a) N. Svenstrup, K. M. Rasmussen, T. K. Hansen, J. Becher, *Synthesis* **1994**, 809–812; b) L. Binet, J. M. Febre, C. Montginoul, K. B. Simonsen, J. Becher, *J. Chem. Soc. Perkin Trans. 1* **1996**, 783–788.

[20] a) M. Takata, B. Umeda, E. Nishibori, M. Sakata, Y. Saito, M. Ohno, H. Shinohara, *Nature* **1995**, *377*, 46–48; b) M. Takata, E. Nishibori, M. Sakata, *Z. Kristallogr.* **2001**, *216*, 71–86.

[21] S. Ishibashi, T. Tamura, S. Tanaka, M. Kohyama, K. Terakura, unpublished results.

[22] P. E. Blöchl, *Phys. Rev. B* **1994**, *50*, 17953–17979.

[23] N. A. W. Holzwarth, G. E. Matthews, R. B. Dunning, A. R. Tackett, Y. Zeng, *Phys. Rev. B* **1997**, *55*, 2005–2017.

[24] G. Kresse, D. Joubert, *Phys. Rev. B* **1999**, *59*, 1758–1775.

[25] J. P. Perdew, K. Burke, M. Ernzerhof, *Phys. Rev. Lett.* **1996**, *77*, 3865–3868.

[26] S. G. Louie, S. Froyen, L. Cohen, *Phys. Rev. B* **1982**, *26*, 1738–1742.

[27] C. Rovira, J. J. Novoa, J.-L. Mozos, P. Ordejón, E. Canadell, *Phys. Rev. B* **2002**, *65*, 081104/4.

[28] S. Ishibashi, K. Terakura, A. Kobayashi, *J. Phys. Soc. Jpn.* **2008**, *77*, 024702/5.

[29] H. Seo, S. Ishibashi, Y. Okano, H. Kobayashi, A. Kobayashi, H. Fukuyama, K. Terakura, *J. Phys. Soc. Jpn.* **2008**, *77*, 023714/4.

Received: January 5, 2009
Published Online: March 23, 2009

